Cardiovascular Research 1990; 24: 447–455

Quantitative ultrasonic assessment of normal and ischaemic myocardium with an acoustic microscope: relationship to integrated backscatter

Kiran B Sagar, Diane H Agemura, William D O'Brien Jr, Lorie R Pelc, Theodore L Rhyne, L Samuel Wann, Richard A Komorowski, David C Warltier

Abstract

Purpose of investigation – The aim was to study ultrasonic propagation properties of normal and ischaemic myocardium with a scanning laser acoustic microscope and to correlate these changes with ultrasonic backscatter.

Design – Myocardial ischaemia was produced by total occlusion of left anterior descending coronary artery in anaesthetised open chest dogs. Myocardium supplied by left circumflex coronary artery served as normal control. IBR5, an optimum weighted frequency average (4-6.8 MHz) of the squared envelope of diffraction corrected backscatter, was measured in vivo. Ultrasonic attenuation coefficient, an index of loss per unit distance, the propagation speed and heterogeneity index were measured from normal and ischaemic regions with a scanning laser acoustic microscope which operates at 100MHz in vitro. Myocardial water content of normal and ischaemic myocardium was also estimated.

Subjects – Were five anaesthetised mongrel dogs.

Results – Attenuation coefficient of 33.8(SD4.2) $dB \cdot mm^{-1}$ in the ischaemic tissue was lower than 63.8(17.2) $dB \cdot mm^{-1}$ in the normal tissue ($p<0.01$). Ultrasonic speed was lower in ischaemic than normal myocardium at 1584(25) *v* 1612(35) $m \cdot s^{-1}$ ($p<0.05$). Heterogeneity index of 11(7) $m \cdot s^{-1}$ in the ischaemic region was lower than 14(8) $m \cdot s^{-1}$ in the normal region (27% reduction, $p<0.05$). IBR5 and myocardial water content were higher in the ischaemic than the normal myocardium: −37.2(SEM1.8) dB *v* −46.6(0.6) dB, ($p<0.01$) and 80.9(0.0)% *v* 78(0.2)%, ($p<0.05$) respectively.

Conclusion – Ultrasonic properties of the myocardium are significantly altered during acute ischaemia.

Conventional echocardiography relies on specular reflection of ultrasound occurring at a tissue interface to depict structures such as myocardium, valves and great vessels.[1] Regions of brightness, speckling and changes in grey scale have been noted in old myocardial infarction, amyloid heart disease, and idiopathic hypertrophic cardiomyopathy.[2–4] Unfortunately, these observations are highly dependent upon subjective alterations in grey scale of the image by the observer as well as by uncontrolled variations in instrumentation. Ultrasonic tissue characterisation quantitatively defines physical state of cardiac muscle with ultrasonic parameters that relate to structural components of cardiac muscle.[5] Ultrasonic propagation properties of biological materials, particularly the attenuation coefficient, are strongly affected at the macromolecular level.[6–8] Four tissue constituents that are of particular importance acoustically are water, protein, collagen, and fat. A comparison of ultrasonic absorption, attenuation, and speed with the concentrations of these tissue constituents has suggested that the ultrasonic propagation properties of tissue can be modelled as functions of the constituent concentrations.[9 10]

Myocardial ischaemia not only results in loss of structural integrity but also results in biochemical alterations including an increase in myocardial lipid and water content.[11 12] The present study characterises ultrasonic propagation properties of normal and ischaemic myocardium with a scanning laser acoustic microscope (SLAM)[13–15] and correlates these changes with ultrasonic backscatter. In comparison to conventional clinical ultrasonoscopes which utilise a frequency of 2 to 5 mHz with a resolution of 1 to 2 mm, the laser acoustic microscope operates at an ultrasonic frequency of 100 mHz and permits assessments of ultrasonic properties of tissues

Medical College of Wisconsin, Department of Medicine, Division of Cardiology, 8700 West Wisconsin Avenue, Milwaukee, Wisconsin 53226, USA
K B Sagar
L R Pelc
L S Wann
R A Komorowski
D C Warltier
University of Illinois, Urbana, USA
D H Agemura
W D O'Brien
Marquette Electronics Inc, Milwaukee, USA
T H Rhyne

Correspondence to: Dr Sagar

Key words: tissue characterisation; myocardial ischaemia; laser acoustic microscope.

Submitted 28 July 1989
Accepted 16 February 1990

at a microscopic level of resolution of approximately 20 μm.

The evaluation of mechanisms responsible for the ultrasonic backscatter in the 2-5 MHz frequency range must be studied with higher frequency ultrasonic energy, ie, acoustic microscopy, since the acoustic scattering results from acoustic inhomogeneities. There is no well founded theory which relates clinical ultrasound signals, which depend on processing backscattered signals, with the scanning laser acoustic microscope, which depends on through transmission. However there are theories which may have laid a foundation for such comparisons. Sehgal and Greenleaf[16] have described a model beginning with a multiple scattering assumption and resulting in methods of characterising tissue properties such as velocity fluctuation and correlation length. The velocity may be related to the ultrasound properties measured with scanning laser acoustic microscopy.

Methods

ANIMAL PREPARATION

Five mongrel dogs of either sex weighing 20-30 kg were anaesthetised with sodium pentobarbitone (30 mg·kg^{-1} intravenously) and ventilated (Harvard Model 607). Atelectasis was prevented by maintaining an end expiratory pressure of 5-7 cm of water with a trap. Po_2, Pco_2 and pH were maintained at physiological levels. Body temperature was controlled at 38°C with a heating pad and servomechanical controller. Phasic and mean aortic blood pressures were recorded via a catheter inserted into the right femoral artery, advanced to the ascending thoracic aorta and connected to a strain gauge pressure transducer (Statham P50). The right femoral vein was cannulated for drug administration.

A thoracotomy was performed in the left fifth intercostal space, the lungs gently retracted, and the heart suspended in a pericardial cradle. Left ventricular pressures were monitored by inserting a pressure transducer tipped catheter (Millar PC380, 8F) into the left ventricle via left carotid artery. The left ventricular pressure pulse was electronically differentiated to obtain peak positive dP/dt. The differentiator was calibrated by means of a triangular waveform of known slope. A 1.0 to 1.5 cm segment of the left anterior descending coronary artery was isolated and a precalibrated electromagnetic flow probe was positioned around the vessels for measurement of coronary blood flow (Statham 2202). A micrometer driven mechanical vascular occluder was placed distal to the flow probe for production of total coronary artery occlusion. The electrocardiogram (limb lead II) and aortic blood pressure were recorded continuously on a Grass (Model 7) polygraph.

Regional myocardial contractile function (segment shortening) was measured in the perfusion territory of the left anterior descending coronary artery by a pair of piezoelectric crystals. The crystals were inserted approximately 10-15 mm apart and 7-10 mm deep within the left ventricular free wall in a circumferential plane parallel to the expected subendocardial muscle fibre orientation. Subsequently, the crystals were secured with a single suture, and the depth of each, average 8.8(SD1.0) mm, was verified at the completion of the experiment. The leads of each crystal were connected to an amplifier that transformed the sound pulse transmitted between the two crystals into an electronic signal proportional to the distance between the crystals. The tracings were monitored on a Soltec oscilloscope (Model 520). Diastolic segment length was determined as the distance between the two crystals at the beginning of the rising phase of positive dP/dt (onset of isovolumetric contraction), and systolic segment length was measured at peak negative dP/dt. The diastolic and systolic segment lengths were normalised to a control value of 10 for the initial diastolic segment length by the method of Theroux *et al.*[17] Percent segment shortening (%SS) was calculated from the equation: %SS = (DL − SL)/DL × 100, where DL is the diastolic and SL is the systolic segment length. The piezoelectric crystals were disconnected during ultrasonic backscatter data acquisition to avoid any potential interference.

Myocardial tissue water was determined by the wet weight/dry weight ratio. Tissue specimens from normal and ischaemic zones were weighed and dried to a constant weight at 95°C in tared vials.

SCANNING LASER ACOUSTIC MICROSCOPE

Operational details of the scanning laser acoustic microscope have been published previously.[13–15] Briefly, the microscope (fig 1) operates in three modes. The first mode is similar to the light microscope. Laser light is used to scan, in a raster fashion, a specimen on the microscope stage which has been surrounded by

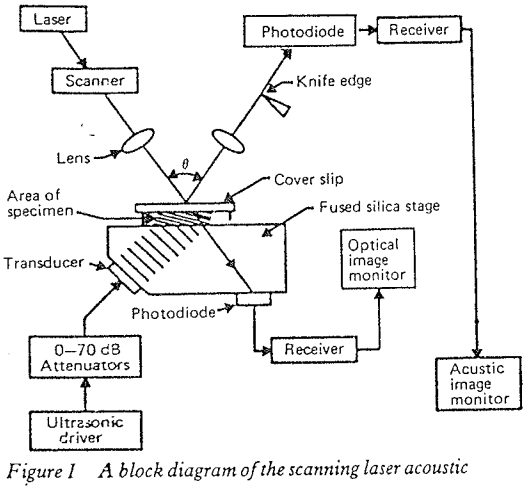

Figure 1 A block diagram of the scanning laser acoustic microscope.

normal saline and covered by a partially mirrored cover slip. Laser light passes through the specimen and is collected subsequently by a photodetector, electronically processed, and transmitted to a television monitor where the magnified (77 times) optical image can be observed (fig 2a).

In the second mode, an acoustic image is created by a piezoelectric transducer operating at 100 MHz beneath the microscope stage, transmitting sound waves through the specimen and incident upon the lower surface of the partially mirrored cover slip. The acoustic energy incident upon the lower surface of the cover slip thus contains the acoustic image information resulting from the inhomogeneous pathway traversed by the wave in passing through the tissue specimen. Minute disturbances at the lower surface of the cover slip are detected by the scanning laser beam. Since the lower surface of the optically transparent cover slip is partially mirrored, a portion of the laser light is reflected from the surface of the cover slip and collected by a second photodetector. This signal is also electronically processed, and an acoustic image (fig 2b) is displayed on a second television monitor. Thus this instrument is capable of producing simultaneous real time acoustic and optical images.

In the third mode (fig 2c) an electronic reference signal is added to the acoustic image signal allowing for determination of the phase of the acoustic signal which has passed through the specimen. The interference mode provides the information necessary to determine, at the microscopic level of the structure, variation in speed of propagation of acoustic energy, ie, the heterogeneity index through the specimen.[13]

Speed is calculated from the magnitude of horizontal shift in the vertical lines (fig 2c). The interference lines shift to the right as they move from a solution of known ultrasonic speed (saline) into the higher speed myocardial tissue and then back to the left during re-entrance into the reference solution. The interference image is digitised and stored in a computer. Each interference line is processed by the computer to yield the ultrasonic speed within the region of interest. For each of three thicknesses of myocardium, a mean ultrasonic speed was determined. The individual mean values were then averaged to yield the ultrasonic speed in meters per second. The advantage of determining the ultrasonic speed using the speed profile is that many speed values, each representative of a different area of the field of view, are obtained. The variation in the spatial speed distribution can then be used as an indication of heterogeneity index of the specimen.

The attenuation coefficient is measured by the insertion loss method,[15] which involves the comparison of two signal amplitudes received from the acoustic image, one with and the other without a specimen of known thickness inserted in the sound path. Insertion loss (IL) is represented as a logarithmic function of the ratio of these two signal amplitudes and provides a quantitative index (in dB) of the ultrasonic energy loss through the specimen. Three or four insertion loss values were recorded for each of the three specimen thicknesses. The slope of the insertion loss v thickness curve, determined by a least squares analysis, yielded the attenuation coefficient in $dB \cdot min^{-1}$.

Uncertainty in the scanning laser acoustic microscope assessment of wave speed and attenuation coefficient was determined for solutions of known acoustic properties and duplicate samples of skin and healing wound tissue. The details of these measurements have been reported previously.[18] Using a homogeneous medium, the accuracy (proximity to the true value) was $\pm$ 2.9%, and the precision (reproducibility of successive independent measurements) was $\pm$ 0.4% for speed; and for attenuation coefficient accuracy and precision were $\pm$ 12% and $\pm$ 15%, respectively. Using heterogeneous samples of normal skin and wound tissue, the speed and attenuation coefficient precisions were $\pm$ 1.7% and $\pm$ 16%, respectively.

ULTRASONIC BACKSCATTER INSTRUMENTATION AND DATA ANALYSIS

Ultrasonic backscatter was measured with a research instrument,[19–24] the CTC-II (Marquette Electronics), which was described previously.[23] The instrument consists of a computer automated ultrasonic transmitter-receiver, plus ECG monitor. The transmitted signals consisted of carrier bursts of 2 μs duration at the five carrier frequencies of 4.5, 5.0, 5.5, 6.0 and 6.5 MHz, together making up a frequency scan. Six frequency scans were performed at evenly spaced intervals over the cardiac cycle, as selected by the computer using the ECG waveform.

A 6 mm unfocused transducer fitted with a 2 cm water filled fixture closed by a finger cot was used. The hand held fixture with transducer was applied directly to the epicardium. By observing A-mode echo patterns, range gates were positioned to encompass the entire myocardial wall. At each sampling site, frequency scans over approximately 16 cardiac cycles were automatically performed and the digitised echoes, together with ECG waveform and various instrument settings, were recorded on floppy disks.

The data containing the frequency scan echoes, instrument settings, and ECG waveforms were analysed using a computer. The automatic phase annotation for each frequency scan was checked by overreading the annotated ECG waveform. As previously,[20] we adjusted the frequency scan echoes for several known effects. Firstly, the magnitude of all echo signals was scaled by adjusting for: (a) transmitter level, and (b) receiver gain setting so as to remove the effect of these instrument settings. Additionally, we adjusted the magnitude of the echo signals as a function

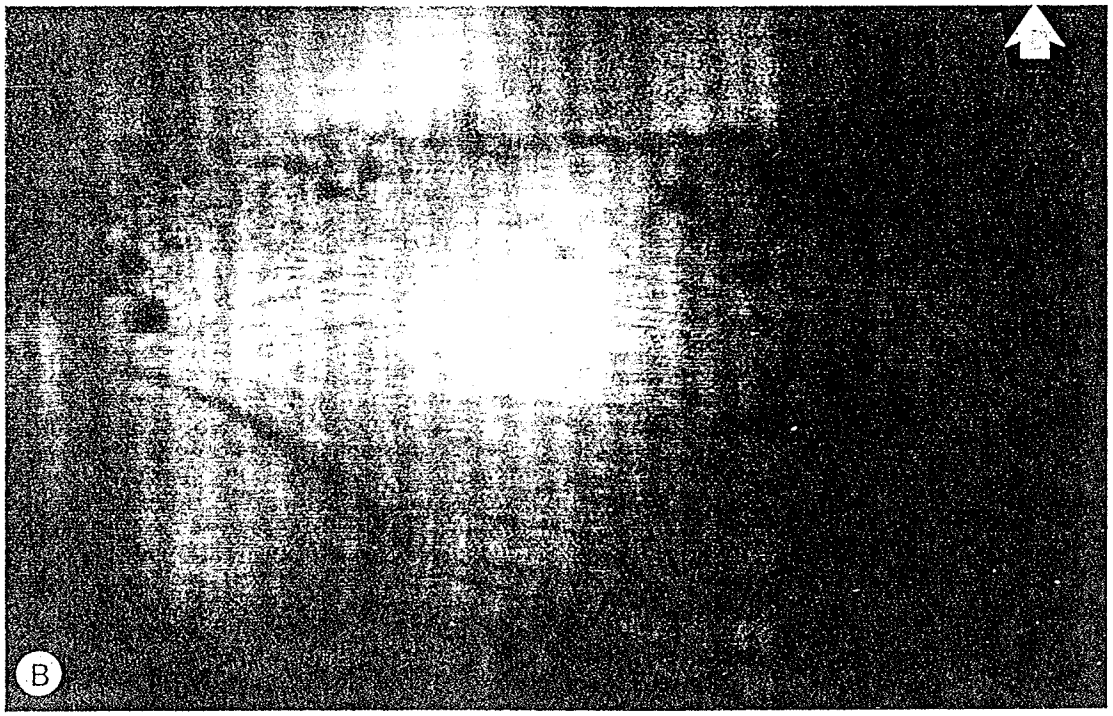

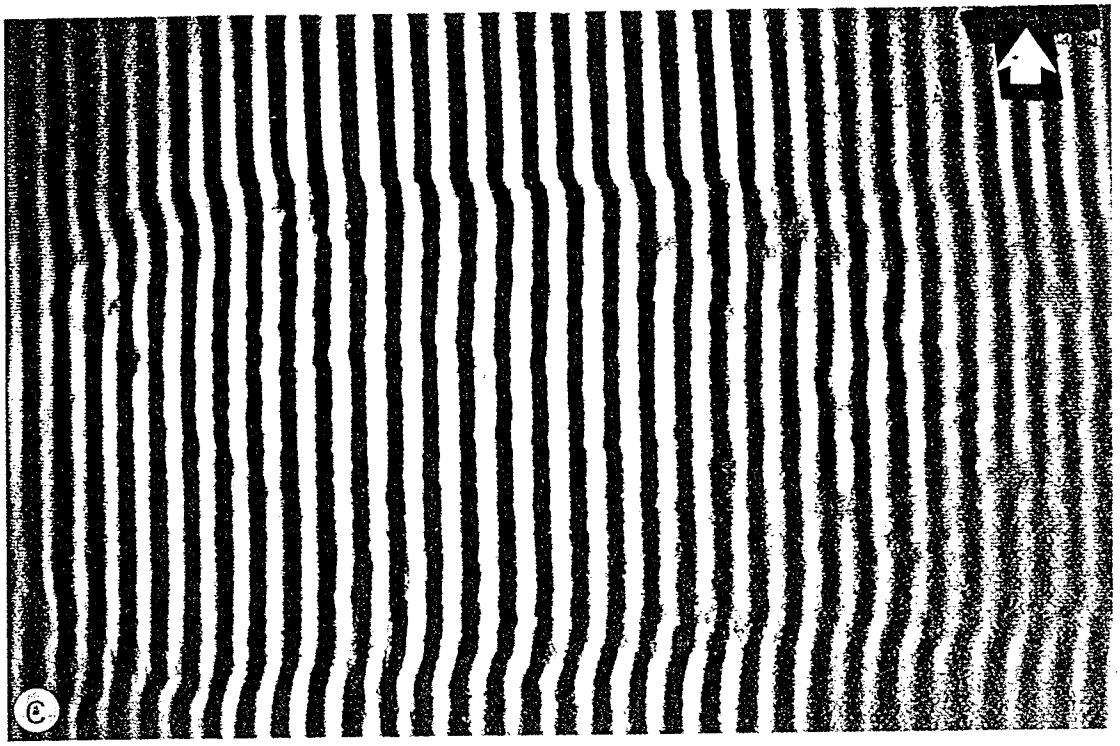

Figure 2 A. An example of the optical image of the unstained frozen section 100 μm thick. B. An example of the acoustic image which contains the attenuation coefficient data. The darker areas represent areas of greater acoustic attenuation. C. An interferogram from which ultrasonic speed is calculated. Speed is calculated from the magnitude of the horizontal shift in the vertical lines. A shift from left to right represents an increase in velocity and vice versa.

of their frequency to correct for four known filters: (1) the transducer frequency calibration, (2) the bulk tissue absorption, (3) the Rayleigh scattering spectrum of the tissue, and (4) the beam diffraction (which was calibrated using a suspension of microspheres[20] to a precision of approximately ± 1dB). This procedure corrected the frequency scan echoes so that they individually have an absolute reflection magnitude and a perfectly flat frequency content (whitened spectrum). Next, the five echo signals from each frequency scan, each with a resolution of 2 μs (a bandwidth of 0.5 MHz), were combined coherently to form a high resolution echo signal (a resolution of 0.5 μs and a bandwidth over 2 MHz). The Integrated Backscatter Rayleigh Five MHz (IBR5) was formed by averaging the squared magnitudes of high resolution echoes at selected ranges. The magnitude was expressed (after averaging) in dB as an absolute measure of the backscatter in cm^2 of reflecting material per cm^3.[20]

The subendocardial region was analysed by averaging successive data points from the high resolution echo over a 1 μs interval (approximately 0.77 $mm \cdot \mu s^{-1}$ time of flight). Taking into account the 0.5 μs resolution of the echoes, this represented two samples each 0.39 mm in duration, which were spaced 0.77 mm apart. (The large epicardial wall echo was automatically tracked and positioned in the subendocardial region to begin 5.4 mm from the epicardial surface.) At each data site, 16 cardiac cycles were recorded with six frequency scans per beat. The mean IBR5 represented averaging over all data taken at that site and for the selected range.

SPECIFIC EXPERIMENTAL PROTOCOL

Acute myocardial ischaemia was produced by total occlusion of the left anterior descending coronary artery for 5 h (n=5). Presence of acute myocardial ischaemia was documented by loss of systolic segment shortening and subsequent electronmicroscopic examination of the tissues. IBR5, systolic segment shortening, and systemic haemodynamic variables were recorded before and after 5 h of coronary artery occlusion. At the end of each experiment, the dog was killed and tissue specimens (5 mm × 5 mm) from the subendocardium of the left anterior descending and left circumflex coronary artery perfusion territories were obtained for scanning laser acoustic microscope study, electron microscopic examination, and determination of myocardial water content.

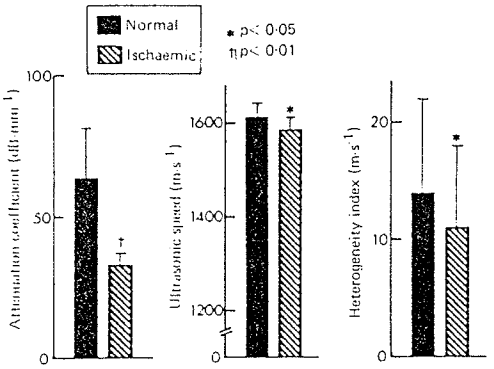

Figure 3 Scanning laser acoustic microscope parameters of normal and ischaemic myocardium. Columns are means, bars=SD.

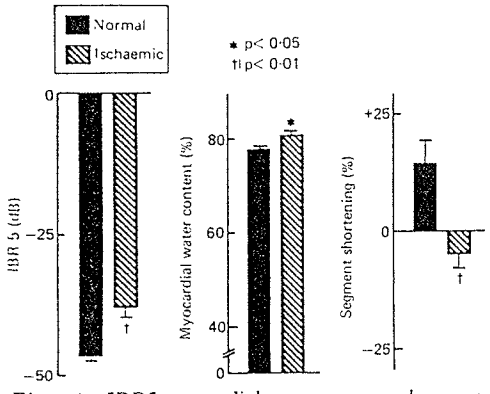

Figure 4 IBR5, myocardial water content, and segment shortening of normal and ischaemic myocardium. Columns are means, bars=SEM.

The acoustic microscope samples were mounted on a circular cork (22 mm diameter, 3 mm thickness) with Ames , Tissue-Tek® OCT (optimal cutting temperature), a polyvinyl alcohol, benzalkonium chloride and polyethylene glycol gel used as an embedding medium for frozen tissue specimens, frozen in liquid nitrogen, placed in Ziploc bags and shipped on dry ice from the Medical College of Wisconsin to the Bioacoustics Research Laboratory at the University of Illinois for storage at −70°C prior to analysis. Specific orientation of the endocardial and epicardial surfaces was carefully marked on the corks. Immediately before ultrasonic analysis, each tissue specimen was removed from the freezer, and the corks were mounted on an object disk of a Lipshaw cryostat (maintained at −35°C). Approximately 50-100 μm of the upper surface of the specimen was sectioned and discarded to provide a flat even surface for subsequent sections. This procedure assured that all specimens remained frozen between the time of initial freezing and the acoustic microscope analysis. Previous studies have shown that rapid freezing in liquid nitrogen has no effect on the ultrasonic impedance and other mechanical properties of several different tissues.[25 26]

Specimens of known thickness (100, 125 and 150 μm) were mounted on a 2.5 cm^2 sheet of mylar (25 μm thick) with albumin fixative so that the position of the endocardium was always known.

STATISTICAL ANALYSIS

All laser acoustic microscopy values and myocardial water concentration values are reported as mean (SD). IBR5 values are reported as mean (SEM). Comparisons between normal and ischaemic myocardium were performed with a paired t test and changes were considered significant when the probability (p) values were less than 0.05.

Results

IBR5, systemic haemodynamic variables and regional segment shortening were measured in each of the five dogs. A total of 10 ischaemic and 10 normal tissue specimens, two from each dog, were analysed with scanning laser acoustic microscopy. Myocardial water was determined from five normal and five ischaemic myocardial tissue samples (one from each dog).

The acoustic microscope ultrasonic propagation properties from the normal and ischaemic regions are illustrated in fig 3. The most dramatic difference between the normal and ischaemic myocardium occurred in the attenuation coefficient. Attenuation coefficient of 33.8(SD 4.2) dB·mm^{-1} in the ischaemic tissue was significantly lower than 63.8(17.2) dB·mm^{-1} in the normal tissue ($p<0.01$). Irreversible tissue damage appeared to have a smaller effect on the ultrasonic speed and heterogeneity index but both also showed a consistent reduction. Ultrasonic speed was 1612(35) m·s^{-1} in the normal and 1584(24) m·s^{-1} in the ischaemic myocardium ($p<0.05$). Similarly, the heterogeneity index of 14(8) m·s^{-1} of normal myocardium was significantly higher than the value of 11(7) m·s^{-1} observed in the damaged tissue.

IBR5, myocardial water concentration, and segment shortening of normal and ischaemic myocardium are summarised in fig 4 and the table. IBR5 in the ischaemic zone was significantly higher than in normal regions at −37.8(SEM 1.8) v −46.6(0.6) dB. Myocardial water concentration was also increased in damaged tissue (80.9±0.6%) compared to normal

IBR5, myocardial water content, and segment shortening for normal and ischaemic samples. Values are means (SEM)

	IBR5 (dB)	Myocardial water content (%)	Segment shortening (%)
Normal	−46.6(0.6)	78.0(0.2)	1.5(5)
Ischaemic	−37.8(1.8)	80.9(0.6)	−5(2)
	p<0.01	p<0.01	p<0.01

IBR5 = Integrated Backscatter Rayleigh 5 MHz, see Methods

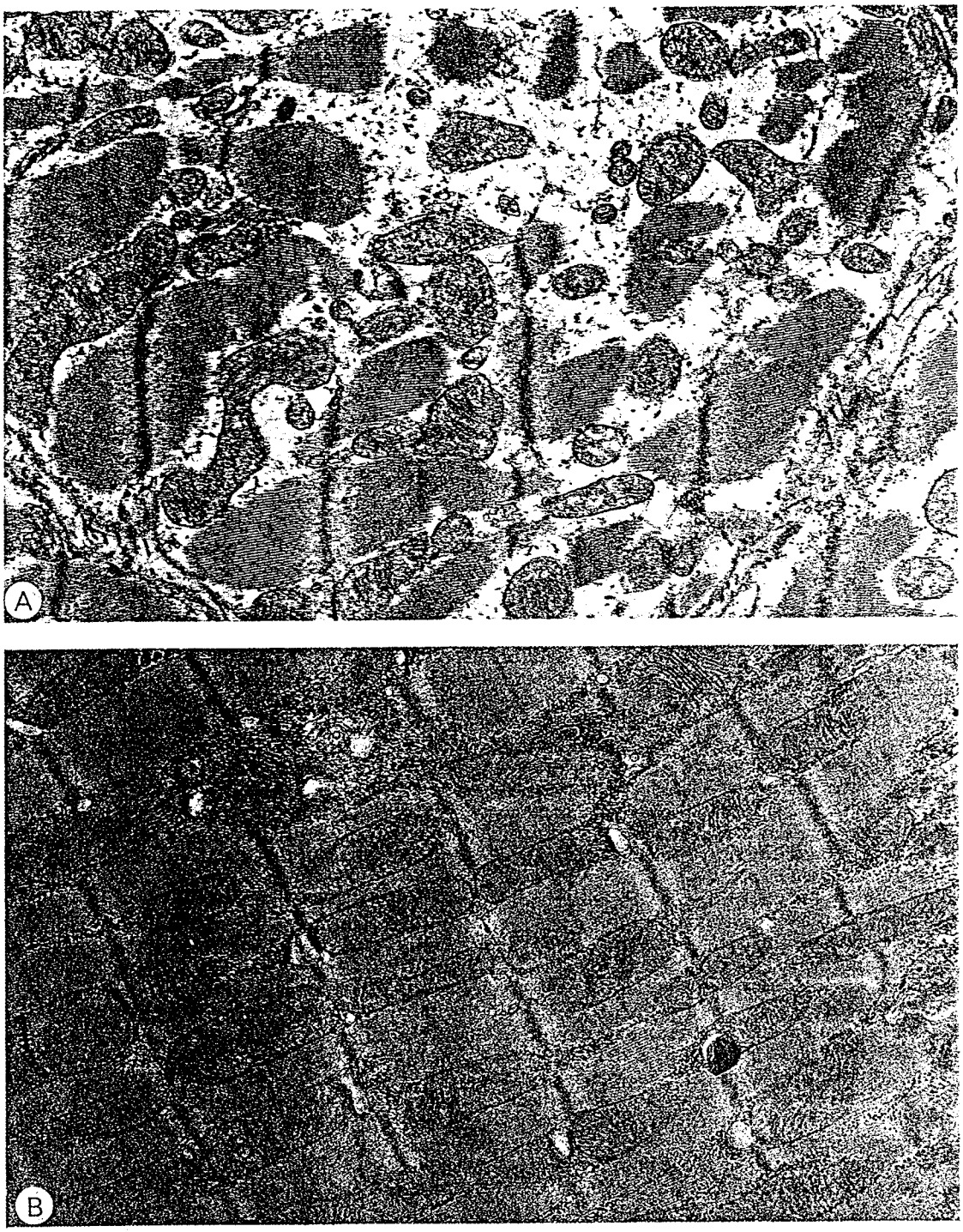

Figure 5 *A. Electronmicroscopic examination of myocardium after 5 h ischaemia shows swelling of myofibrils, mitochondria and depletion of glycogen (x 12 000). B. Normal myocardium shows intact myofibrils, mitochondria and abundant interfibril glycogen (x 15 000).*

tissue, at 80.9(0.6) *v* 78(0.2)%. Segment shortening was measured in the territory of left anterior descending coronary artery before and after the total occlusion. Segment shortening of 15(5)% in the left anterior descending region was replaced by aneurysmal bulging of −5(2)% during total coronary artery occlusion.

Light microscopic features of the ischaemic and the normal myocardium were identical after 5 h of ischaemia. At the ultrastructural level, changes were apparent in the ischaemic myocardium (fig 5a). Myofibrils were swollen. There was an increase in interstitial tissue. There was loss of mitochondrial crystae and mitochondrial swelling, along with an absence of intermyofibril glycogen. In contrast, the control tissue (fig 5b) showed no swelling of myofibrils. The myofibrils were lined by mitochondria with prominent crystae, and interfibril glycogen was abundant.

Discussion

The present investigation shows that irreversible tissue damage produces a decrease in attenuation coefficient, ultrasonic speed, and heterogeneity index as measured by the scanning laser acoustic microscope and this is associated with an increase in integrated backscatter and myocardial water concentration.

It has been known for decades that the ultrasonic propagation properties, particularly the attenuation coefficient, of biological materials are strongly affected at the macromolecular level.[6–8] Four tissue constituents that are of particular importance acoustically are water, protein, collagen, and fat. A comparison of ultrasonic absorption, attenuation and speed to the concentrations of these tissue constituents has suggested that the ultrasonic propagation properties of tissue can be modelled as functions of the constituent concentrations.[9 10]

Tissue water concentration is inversely related to attenuation coefficient[27–30] and propagation speed[27 28 31 32] of ultrasound in human liver and brain, rabbit liver, and canine wound. Thus in general the higher the tissue water concentration, the lower the attenuation coefficient and speed. An exception to this has been reported[32] in excessively fatty rat livers wherein speed increases with increasing water concentration. Here the excessive increase in lipid concentration (up to 27% wet weight basis) replaces water (correlation coefficient of −0.82 between lipid and water concentrations). No suggestion about the cause of this marked difference was reported.

Collagen, lipid and protein concentrations also appear to play an important role in the determination of tissue attenuation coefficient and speed. The high tensile strength of collagen[33] would suggest increased attenuation coefficient and speed, which indeed is the case for speed of mouse tendon thread[34] and for attenuation coefficient and speed of canine wound[28] and human liver.[35] Tissue lipid concentration is proportional to attenuation coefficient in human liver[35–37] and rat liver,[38] and inversely proportional to speed in rat liver.[29 37] Proteins seem to be responsible for the largest part of the observed tissue attenuation, although no clear dependencies between tissue protein concentration and ultrasonic propagation properties have emerged.[39]

Prolonged myocardial ischaemia results in cellular swelling with enlarged sarcoplasmic spaces, disruption of sarcolemmal membrane, and mitochondrial fragmentation.[12] Increased water[12] as well as loss of protein synthesis[40] also occurs following prolonged ischaemia. Increased myocardial water appears to be the dominant tissue change which could explain the reduction in the attenuation coefficient and speed. The increased lipid concentration could also be responsible for part of the reduction in speed.

In normal skin and wound tissues studies,[41] the heterogeneity index has been shown to be predominantly dependent on tissue collagen and water concentrations, where heterogeneity index correlated inversely with water and positively with collagen. For canine tissue the heterogeneity index of normal cardiac tissue is greater than that of acutely infarcted tissue, when the tissue water concentration increases, thus also showing an inverse relationship between heterogeneity index and water. Even though collagen concentration was not determined, it is possible to speculate that the collagen concentration decreased since water concentration was known to increase. Therefore, extending the speculation, heterogeneity index was directly related to collagen concentration, a similar observation to that of canine skin tissue.

Infarcted myocardium shows an increase in ultrasonic backscatter.[5 23] This increase has been associated with loss of structural integrity and increases in myocardial water.[42] These changes may alter the size of ultrasonic scatterers, although the exact nature of scatterers still remains unknown.

Theoretically, a strong relationship exists between IBR5 and heterogeneity index. IBR5 is related to tissue architecture and mathematically can be related to spatial variations in compressibility and density. Ultrasonic speed is inversely related to the square root of density times compressibility. Therefore heterogeneity index which quantitatively describes the distribution of speed variation can be a useful index to describe the degree to which ultrasound scatters. One can speculate that acute ischaemia causes the myocardium to become more inhomogeneous, which in turn results in increased backscatter. In the present study, an increase in IBR5 was observed during ischaemia but no corresponding increase in heterogeneity index was noted. This can be explained by the fact that compressibility and density change in a similar fashion and no significant change occurs in ultrasonic speed and heterogeneity index.

In this study, the interaction of ultrasound with normal and ischaemic myocardium has been characterised in a unique fashion with the aid of the scanning laser acoustic microscope. For the first time, the ultrasonic properties of myocardial tissue have been quantified both in vivo and in vitro. Further research will be necessary in order to develop a sufficient understanding of the ultrasonic tissue signature of myocardium and its promising application in the diagnosis of cardiac pathologies such as amyloidosis and hypertrophy.

Supported by a grant from Marquette Electronics Inc, US Public Health Service Grants HL39014 and HL36144, Cardiovascular Research Training Grant T32 HL07546 and CA36029 (University of Illinois). The authors appreciate the excellent technical assistance of Jeanne Howard and the secretarial assistance of Tammy Jo Wells.

1 Feigenbaum H. *Echocardiography*. Philadelphia: Lea and Febiger, 1986.
2 Rasmussen S, Clorya BD, Feigenbaum H, Knoebel SB. Detection of myocardial scar tissue by M-Mode echocardiography. *Circulation* 1978;57:230–7.
3 Bhandari AF, Nanda NC. Myocardial texture characterization by two-dimensional echocardiography. *Am J Cardiol* 1988;51:817–25.
4 Martin RP, Rakowski H, French J, Popp RL. Idiopathic hypertrophic subaortic stenosis viewed by wide angle phased array echocardiography. *Circulation* 1979;59:1206–17.
5 Miller JG, Perez JE, Sobel BE. Ultrasonic characterization of myocardium. *Prog Cardiovasc Dis* 1985;28:85–110.
6 Carstensen EL, Li K, Schwan HP. Determination of the acoustic properties of blood and its components. *J Acoust Soc Am* 1953;25:286–9.
7 Carstensen EL, Schwan HP. Acoustic properties of hemoglobin solutions. *J Acoust Soc Am* 1959;50:692–9.
8 Pauly H, Schwan HP. Mechanism of absorption of ultrasound in liver tissue. *J Acoust Soc Am* 1971;50:692–9.
9 O'Brien WD. The relationship between collagen and ultrasonic attenuation and velocity in tissue. In: *Ultrasonic international*. Guildford, Surrey, UK: IPC Science and Technology Press, 1977:194–205.
10 Pohlhammer J, O'Brien WD. The relationship between ultrasonic attenuation and speed in tissues and the constituents: water, collagen, protein and fat. In Fullerton GD, Zagzebski, eds. *Medical physics of CT and ultrasound: tissue imaging and characterization*. New York: American Institute of Physics, 1980:409–35.
11 Bilheimer DW, Buja LM, Parkey RW, Bonte FJ, Willerson JT. Fatty acid accumulation and abnormal lipid deposition in peripheral and border zones of experimental myocardial infarcts. *J Nucl Med* 1978;19:276–83.
12 Basuk WL, Reimer KA, Jennings RB. Effect of repetitive brief episodes of ischemia on cell volume, electrolytes and ultrastructure. *J Am Coll Cardiol* 1986;8:33–41.
13 Embree PM, Tervola KMU, Foster SG, O'Brien WD. Spatial distribution of the speed of sound in biological materials with the scanning laser acoustic microscope. *IEEE Trans Sonics Ultrason* 1985;SU-32:341–50.
14 Tervola KMU, O'Brien WD. Spatial frequency domain technique: an approach for analysing the scanning laser acoustic microscope interferogram images. *IEEE Trans Sonics Ultrason* 1985;SU-32:544–54.
15 Tervola KMU, Foster SG, O'Brien WD. Attenuation coefficient measurement technique at 100 MHz with the scanning laser acoustic microscope. *IEEE Trans Sonics Ultrason* 1985;SU-32:259–65.
16 Sehgal CM, Greenleaf JF. Scattering of ultrasound by tissues. *Ultrasonic Imaging* 1984;6:60–80.
17 Theroux P, Franklin D, Ross J, Kemper WS. Regional myocardial function during acute coronary occlusion and modification by pharmacologic agents in dogs. *Circ Res* 1972;35:896–902.
18 Steiger DL, O'Brien WD, Olerud JE, Riederer-Henderson MA, Odland GF. Measurement uncertainty assessment of the scanning laser acoustic microscope and application to canine skin and wound. *IEEE Trans Ultrasonics, Ferroelectrics and Frequency Control* 1988;35:741–8.
19 Rhyne TL. *Acoustic instrumentation and characterization of lung surface*. London: John Wiley and Sons, Research Studies Press, 1977.
20 Rhyne TL, Sagar KB, Wann LS, Haasler G. The myocardial signature: absolute backscatter, cyclic variation, frequency variation and statistics. *Ultrasonic imaging* 1986;8:107–20.
21 Rhyne TL, Sagar KB, Wann LS, Haasler G. A myocardial backscatter parameter with maximal sensitivity to cyclic variation. *Proc Ultrasonic Symp, IEEE* 1986; Cert No 86H23775-4:909.
22 Sagar KB, Pelc L, Rhyne TL, Wann LS, Warltier DC. Influence of heart rate, preload, afterload and inotropic state on integrated backscatter. *Circulation* 1988;77:478–83.
23 Sagar KB, Rhyne TL, Warltier DC, Pelc L, Wann LS. Intramyocardial variability in integrated backscatter: effects of coronary occlusion and reperfusion. *Circulation* 1987;75:436–42.
24 Sagar KB, Rhyne TL, Greenfield LJ. Echocardiographic tissue characterization and range gated Doppler for diagnosis of pulmonary embolism. *Circulation* 1983;67:365–80.
25 Marangore RD, Glaser AA, Must JS, Brody GS, Beckwith TG, Walker GR, White WL. Effect of storage and handling techniques on skin tissue properties. *Ann NY Acad Sci* 1966;136:439–54.
26 Gellski JV, Shung KK. Studies on acoustic impedance of major bovine blood vessel walls. *J Acoust Soc Am* 1982;71:467–70.
27 Bamber JC, Hill CR, King JA. Acoustic properties of normal and cancerous human liver-II. Dependence on tissue structure. *Ultrasound Med Biol* 1981;7:135–44.
28 Olerud JE, O'Brien WD, Riederer-Henderson MA, *et al*. Ultrasonic assessment of skin and wounds with the scanning laser acoustic microscope. *J Invest Dermatol* 1987;88:615–23.
29 O'Brien WD, Erdman JW, Hebner TB. Ultrasonic propagation properties (@ 100 MHz) in excessively fatty rat liver. *J Acoust Soc Am* 1988;83:1159–66.
30 Kremkau FW, McGraw CP, Barnes RW. Acoustic properties of normal and abnormal human brain. In: Linzer M, ed. *Ultrasonic tissue characterization II*. NBP Publication No 525. Washington DC: US Government Printing Office, 1979:81–4.
31 Wladimisoff JW, Craft JL, Talbert DC. In vitro measurements of sound velocity in human fetal brain tissue. *Ultrasound Med Biol* 1977;1:377–82.
32 Sarvazyan AP, Lyrchilsov AG, Gorelov SE. Dependence of ultrasonic velocity in rabbit liver on water content and structure of the tissue. *Ultrasonics* (in press).
33 Fields S, Dunn F. Correlation of echographic visualizability of tissue with biological compositions and physiological state. *J Acoust Soc Am* 1973;54:809–12.
34 Cross SA, O'Brien WD. Direct ultrasonic velocity measurements of mammalian collagen threads. *J Acoust Soc Am* 1979;65:507–11.
35 Lin T, Ophir J, Potter G. Correlation of ultrasonic attenuation with pathologic fat and fibrosis in liver disease. *Ultrasound Med Biol* 1988;14:729–34.
36 Taylor KJW. Ultrasonic tissue characterization. *Applied Radiol* 1987;16:45–50.
37 Duerinckx A, Rosenberg K, Hoefs J, *et al*. In vivo acoustic attenuation in liver: correlations with blood tests and histology. *Ultrasound Med Biol* 1988;14:405–13.
38 Tervola KMU, Gummer MA, Erdman JW, O'Brien WD. Ultrasonic attenuation and velocity properties is rat liver as a function of fat concentration: a study at 100 MHz using a scanning laser acoustic microscope. *J Acoust Soc Am* 1985;77:307–13.
39 Dunn F, O'Brien WD. Ultrasonic absorption and dispersion. In: Fry FJ, ed. *Ultrasound: its application in medicine and biology*. Amsterdam: Elsevier, 1978:393–439.
40 Kao R, Rannels E, Morgan HE. Effects of anoxia and ischemia on protein synthesis in perfused rat hearts. *Circ Res* 1976; 38:124–33.
41 Steiger DL. Ultrasonic assessment of skin and wounds with the scanning laser acoustic microscope. Urbana, Illinois: University of Illinois, 1981. MS Thesis.
42 Mimbs JW, Bauwens D, Cohen RD, O'Donnell M, Miller JG, Sobel BE. Effects of myocardial ischemia on quantitative ultrasonic backscatter and identification of responsible determinants. *Circ Res* 1981;49:89–96.